Molecular Immunology 48 (2011) 657–669

Contents lists available at ScienceDirect

Molecular Immunology

journal homepage: www.elsevier.com/locate/molimm

Protection against malaria is conferred by passive transferring rabbit F(ab)$_2'$ antibody fragments, induced by *Plasmodium falciparum* MSP-1 site-directed designed pseudopeptide-BSA conjugates assessed in a rodent model

José Manuel Lozano[a,b,*], Liliana Patricia Lesmes[a,b], Gina Marcela Gallego[a], Manuel Elkin Patarroyo[a,b]

[a] *Fundación Instituto de Inmunología de Colombia (FIDIC) and Universidad del Rosario, Bogotá, DC, Colombia*
[b] *Universidad Nacional de Colombia, Bogotá, DC, Colombia*

ARTICLE INFO

Article history:
Received 25 September 2010
Received in revised form 8 November 2010
Accepted 9 November 2010
Available online 4 December 2010

Keywords:
Antibody-(Fab)$'_2$
Neutralizing antibody
Rodent malaria model
Immunotherapy
Synthetic vaccine

ABSTRACT

F(ab)$_2'$-immunoglobulin (Ig) fragments induced by site-directed designed immunogens are emerging as novel tools of potential utility in the treatment of clinical episodes of transmissible diseases such as malaria. Immunogens based on reduced amide pseudopeptides based on site-directed molecular modifications represent structural probes that could be considered as novel vaccine candidates, as we have previously demonstrated.

We have obtained F(ab)$_2'$-Ig rabbit antibodies induced against the *N*-terminal sequence of the native Merozoite Surface Protein-1 (MSP-1) of *Plasmodium falciparum* and a set of five MSP-1-derived reduced amide pseudopeptides. Pseudopeptides were designed for inducing functional neutralizing monospecific polyclonal antibodies with potential applications in the control of malaria. Following a classical enzyme immunoglobulin fractionation, F(ab)$_2'$-Ig fragments were tested for their ability to suppress blood-stage parasitemia by passive immunization in malaria-infected mice. Some of these fragments proved totally effective in suppressing a lethal blood-stage challenge infection and others reduced malarial parasitemia.

These data suggest that protection against *Plasmodium yoelii* malaria following passive transfer of structurally well-defined β-strand F(ab)$_2'$-Ig fragments can be associated with specific immunoglobulins induced by site-directed designed MSP-1 reduced amide pseudopeptides.

1. Introduction

A peptide derived from the *N*-terminal portion of the *Plasmodium falciparum* Merozoite Surface Protein-1 (MSP-1) designated as 1513 (^{42}GYSLFQKEKMVLNEGTSGTA^{61}) has been extensively consider as a candidate component to be included in a multicomponent subunit-based chemically synthesized antimalarial vaccine, in spite of being poorly immunogenic and non-protection inducer against malaria. As has been demonstrated in the research performed in our Institute, critical binding residues of high activity binding peptides (HABPs), has to be identified and strategically substituted. Once the critical binding residues of peptide 1513 were identified by specific receptor-ligand experiments, a rational design allowed us to strategically include site-directed peptide bond isosters, in order to produce a novel class of structural probes (Lozano et al., 1998).

Thus, each peptide bond associated to the ^{48}K-KMV^{52} Red Blood Cell (RBC) binding motif was systematically replaced by a methylene amine ψ-[CH_2NH] isoster bond to generate a family of malarial pseudopeptides.

Pseudopeptide identity and purity were analyzed by Matrix-Assisted Laser Desorption Ionization Mass Spectrometry by the

Abbreviations: F(ab)$'_2$, antibody fragment for antigen binding; HABP, high activity binding peptide; ψ-[CH_2NH], reduced amide isoster bond; MHC, major histocompatibility complex; TCR, T-cell receptor; TCC, T-cell clone; APC, antigen presenting cell; CDR, complimentarily determinant region; HLA, human leukocyte antigens; IL-4, interleulin-4; INF-γ, gamma interferon; mAb, monoclonal antibody; MSA-1 or MSP-1, Merozoite Surface Antigen-1; MSA-2 or MSP-2, Merozoite Surface Antigen-2; RBCs, red blood cells; iRBC, infected red blood cell; CSP, circumsporozoite surface protein; IgM, immunoglobulin-M isotype; IgG, immunoglobulin-G isotype; F(ab)$_2'$, immunoglobulins antigen binding fragment-2; $NaBH(OAc)_3$, triacetoxyborohydride; DMF, *N*,*N*′-dimethylformamide; DCE, dichloroethane; THF, tetrahydrofuran; $NaCNBH_3$, sodium cyanoborohydride; Pd/C, palladium over charcoal; 4-MBHA, 4-methylbenzhydrilamine; *t*-Boc, *tert*-butyloxycarbonyl; Fmoc, 9-fluorenylmethyloxycarbonyl; DIEA, diisopropylethylamine; TFA, trifluoroacetic acid; TFE, trifluoroethanol; m-*R*,*S*-TMD, 2,2,5-trimethyl-1,3-dioxane-4,6-dione; RP-HPLC, reverse-phase high-performance liquid chromatography; [D6]DMSO, deuterated-dimethylsulfoxide; ^{1}H-NMR, proton-nuclear magnetic resonance; CD, Circular Dichroism; NOE, Nuclear Overhauser effect; SPf-66, synthetic *Plasmodium falciparum*-66 vaccine.

* Corresponding author at: Biocatalysis Functional Group, Fundación Instituto de Inmunología de Colombia (FIDIC), Carrera 50 No. 26-20, ZC 020304, Bogotá, Colombia. Tel.: +57 1 481 5219; fax: +57 1 481 5269.
E-mail addresses: jotalozano@gmail.com, jm.lozano@fidic.org.co (J.M. Lozano).

0161-5890/$ – see front matter © 2010 Elsevier Ltd. All rights reserved.
doi:10.1016/j.molimm.2010.11.007

Time Of Flight technique (MALDI-TOF) and analytical Reverse-Phase High-Performance Liquid Chromatography (RP-HPLC), respectively. Previously reported proton-Nuclear Magnetic Resonance (^{1}H NMR) data demonstrated how the secondary structure of this protein fragment was specifically modulated by each isoster bond (Lozano et al., 1998). The immunological properties of each component of this structural family were determined by inducing monoclonal antibodies, which were shown to possess neutralizing properties against *in vitro* malarial infection. In a recent study, we reported that the passive transfer of immunoglobulins directed against reduced amide pseudopeptides derived from a highly conserved sequence of MSP-2, another relevant target for an antimalarial vaccine component. Such experiment demonstrated that passively transferred immunoglobulins protected and delayed onset of malarial infection in BALB/c mice after being experimentally challenged with the *Plasmodium berghei* ANKA strain.

In the present work, we have examined the potential of passively transferring F(ab)$_2'$ antibody fragments induced by MSP1-pseudopeptides. F(ab)$_2'$ fragments were obtained by papain treatment of Ig from rabbit polyclonal mono-specific antibodies induced by pseudopeptide-bovine serum albumin (BSA) conjugates.

The results of the present study demonstrate that F(ab)$_2'$ fragments possess well defined secondary structure patterns, as indicated by Circular Dichroism (CD) experiments, and that such patterns could be associated with a protective effect against malarial infection, as assessed in a rodent animal model challenged with a lethal dose of a *Plasmodium yoelii* 17XL strain.

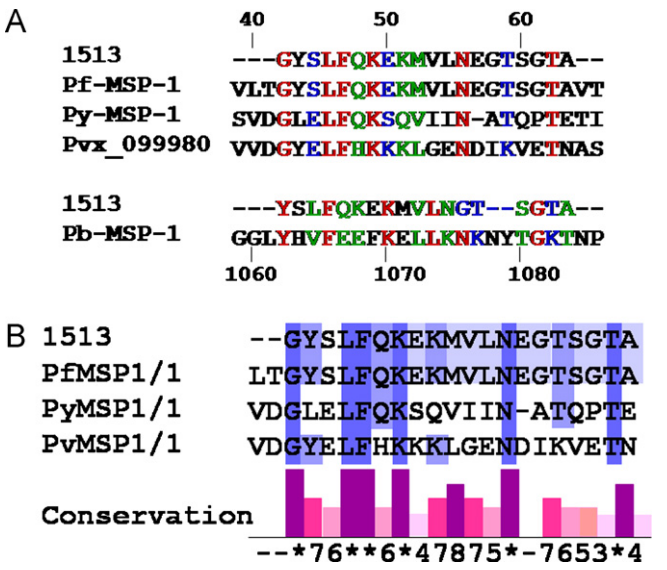

Fig. 1. Structural characteristics of the MSP-1-derived peptide 1513. (A) Alignment of the 1513 peptide sequence (MSP-1$^{42-61}$) and the MSP-1 homolog sequences in *Pf* (*Plasmodium falciparum*), *Py* (*Plasmodium yoelli*) and *Pv* (*Plasmodium vivax*). (B) Degree of sequence identify is represented according to the following color code: 80%, mild blue; higher than 60%, light blue; higher than 40%, light gray and lower than 40%, white. The degree of sequence conservation was analyzed using Jalview-EBI, where the 11* score represents identical amino acids, 8 and 7 conserved amino acids, and 6 and 5 semi-conserved amino acids. (For interpretation of the references to color in this figure legend, the reader is referred to the web version of the article.)

2. Material and methods

2.1. Bioinformatics analysis

The sequence of *P. falciparum* MSP-1 (accession number Pfi1475w) previously reported by Gilson et al. was used as bait for obtaining information about orthologous sequences in other *Plasmodium* species from the *Plasmodb* database (http://plasmodb.org/plasmo/), which were confirmed in the NCBI database (http://www.ncbi.nlm.nih.gov). Such screening allowed us to obtain the codes of the followings orthologous sequences: *Plasmodium vivax* MSP-1 Pvx_099980, *Plasmodium berghei* MSP-1 Pb000172.01.0, *Plasmodium yoelii* MSP-1 Py05748, *Plasmodium chabaudi* MSP-1 Pc000255.03.0 and *Plasmodium knowlesi* pkh_072850.

The MSP-1$^{42-61}$ sequence was aligned using ClustalW available at http://personal.rhul.ac.uk/ujba/110/bioinfo/clustalE.html, to obtain the degree of homology between these sequences. The degree identity and conservation of each residue was then determined using the Jalview Java Alignment Editor (Clamp et al., 2004).

2.2. Synthesis of peptide bond isosters and conjugation to BSA

Based on the primary structure of MSP-1$^{42-61}$ (peptide 1513) shown in Fig. 1A, a set of five reduced amide oligomer pseudopeptides was designed and synthesized. In brief, all molecules were manually synthesized through *tert*-butyloxycarbonyl (*t*-Boc)-based solid-phase peptide synthesis (SPPS), following a protocol first reported by Merrifield (1963) and later modified for multiple peptide synthesis (Houghten, 1985). Each amino acid residue was placed on the pseudopeptide backbone as described elsewhere (Cushman and Oh, 1991; Ho et al., 1993; Sasaki et al., 1987). The ψ-[CH_2NH] surrogate was introduced by deprotected N^{α}-amino group's resin-bound reductive alkylation with the *t*-Boc-protected amino acid aldehyde (0.576 mmol) in DMF containing 0.5% acetic acid (HOAc), followed by portion-wise addition of $NaBH_3CN$ (0.67 mmol) for 40–60 min. Total coupling was checked by the Ninhydrin test and, repeating the coupling reaction when necessary. Coupling was allowed to proceed for 5 h under constant shaking, followed by washes with *N*,*N*′-dimethylformamide (DMF), isopropanol and dichloromethane. Standard solid phase peptide synthesis was carried out to introduce the remaining *t*-Boc amino acids to the last *N*-terminal residue. Protected pseudopeptide-resin batches were treated with trifluoroacetic acid (TFA) and cleaved from the resin by treatment with low concentrations of anhydrous hydrogen fluoride (HF) containing 10% anisole at 0 °C for 60 min. After HF evaporation in an N_2 stream, each pseudopeptide-resin product was washed with cold diethyl ether, then extracted with 5% HOAc and lyophilized. The crude products obtained for each ψ-[CH_2NH] surrogate were further analyzed by analytical RP-HPLC, purified by preparative RP-HPLC and identified by MALDI-TOF mass spectrometry. A full procedure for peptide-based polymer production is described elsewhere (Lozano et al., 1998; Lioy et al., 2001).

Coupling of pseudopeptides to a bovine serum albumin (BSA) was performed by a classical glutaraldehyde treatment. Briefly, equal amounts of each pseudopeptide and BSA were mixed to obtain a 2 mg/mL preparation. Subsequently, small amounts of 0.38% glutaraldehyde dissolved in phosphate buffered saline (PBS) were added to the protein preparation. Protein-peptides were cross-linked to BSA through bonds established between primary amine groups with the aldehyde groups of glutaraldehyde, letting the reaction to elapsed overnight at room temperature under constant shaking to obtain all possible pseudopeptide-BSA conjugates. Then, all conjugates were dialyzed against saline solution to eliminate non-desirable small size complexes, such as pseudopeptide-glutaraldehyde-pseudopeptide.

2.3. Rabbit immunization to obtain polyclonal antibodies

Polyclonal antibodies against each 1513-derived pseudopeptide conjugated to BSA, were employed for by immunizing New Zealand

female rabbits of 5 pounds with each 1513-pseudopeptide-BSA conjugate. Rabbits were obtained from the *Universidad Nacional de Colombia* animal breeding facility. Briefly, rabbits were intramuscularly (i.m.) inoculated six times in the inner face of the posterior leg with 0.5 mL of each 1513-pseudopeptide-BSA conjugate (1 mg/mL), emulsified in Complete Freund's Adjuvant (CFA) (v/v) for the first dose and in Incomplete Freund's Adjuvant (IFA) for the subsequent immunizations. Rabbits were bled from the marginal ear vein before the first immunization and weekly after each immunization to obtain 5–10 mL blood samples.

2.4. Immunoglobulin purification and F(ab)$_2$′ fractionation

In order to obtain anti-pseudopeptide specific antibodies from rabbit serum samples, these were treated for depleting anti-BSA antibodies. Those were removed from all serum samples by absorbing them with increasing amounts of BSA (20–250 mg). Once all samples proven to be free of anti-BSA antibodies, antibodies specific to each pseudopeptide were then selectively precipitated by saturation with 80% ammonium sulfate. After centrifugation, supernatants were carefully removed and precipitated antibodies were reconstituted using 10 mM Tris–HCl pH 8.5 and dialyzed against the same buffer on a Spectra-pore® dialysis membrane (Houston, Texas, USA) at 4 °C.

Weak anionic exchange chromatography (AEC) was performed with the antibody-enriched dialyzed precipitates obtained from reactive rabbit sera, using a DEAE-Sephadex A-25 resin (Pharmacia, Uppsala, Sweden) previously equilibrated with 10 mM Tris–HCl buffer, pH 8.5, and to which antibodies were led to bind at 4 °C overnight under constant shaking. Igs were eluted from the column by progressively increasing the buffer's ionic strength from 50 mM, 100 mM and 500 mM NaCl. A total of 4 column volumes (250 mL) were added per step, collecting 10 mL fractions at a constant flow rate of 0.5 mL/min. The resin was then re-equilibrated with 10 mM Tris–HCl buffer, pH 8.5. All elution fractions were characterized by direct Dot blot for Ig detection and positive fractions were submitted to indirect Dot blot against a *P. falciparum* lysate as well as against each 1513 pseudopeptide. Reactive elution fractions from direct and indirect Dot blots were pooled taking into account the ionic strength order in which they have been eluted. Pooled fractions were subsequently dialyzed against PBS at 4 °C. The purity of each Ig pooled fraction was assessed by sodium dodecyl sulfate polyacrylamide gel electrophoresis (SDS-PAGE). Further characterization was performed to define each Ig pool's reactivity against *P. falciparum* lysate by Western blot.

To obtain pure F(ab)$_2$′-Ig fragments, a controlled papain digestion followed by SDS-PAGE examination was performed as reported elsewhere (Gregory et al., 2003; Kaufmann et al., 2006; Bennett et al., 1997). Briefly, a solution of each previously purified antibody was treated with Cysteine-activated papain. A 0.5 M L-Cysteine solution was obtained by dissolving 33.2 mg in 200 μL of 1N NaOH and 800 μL PBS. For papain activation, 300 μL of this L-Cysteine solution were added to 200 mg of papain suspended in 1 mL PBS, incubating this solution for 30 min at 37 °C. The reaction mixture was poured into a previously packaged DEAE-Sephadex A-25 resin-column equilibrated with 0.1 M Acetate/0.003 M EDTA buffer, pH 5.5 (column volume = 11.42 mL). Ten 1-mL fractions were collected and kept refrigerated until use. Protein concentration was determined by the bicinchoninic acid (BCA) micro-assay, as described in the next section. Normally, activated papain concentrations ranged around 2.30 mg/mL and eluted in fractions 8–10. From one of these fractions, Ig samples previously dialyzed against the same buffer were incubated with 1 mL for 14 h at 37 °C under constant shaking to allow total fractionation of each Ig. The digestion reaction was stopped by adding either 4.7 mg/mL of 50 μL iodoacetamide or 50 μL of 1 M H_3PO_4. Ig digestion was examined by 10% SDS-PAGE. The protein mixture was dialyzed against PBS, pH 8.0, and then concentrated with saccharose using a 6000–8000 Da MWCO Spectra-pore® dialysis membrane (Houston, TX, USA), according to a protocol described elsewhere (Martínez et al., 2009).

In order to separate F(ab)$_2$′ fragment from Ig Fc portions, the reaction mixture was poured onto a 11.94-mL Protein-A Sepharose CL-4B column (Pharmacia, Upsala, Sweden). F(ab)$_2$′ fragment were eluted using 0.1 M citric acid buffer solutions adjusted to pH 6.5, pH 4.5 and pH 3.0, respectively, by adding 1 M NaOH as needed. In each step, twelve 1-mL elution fractions were carefully collected, neutralizing the pH with 50 μL of 1 M Tris–HCl pH 9–10. Protein concentration was analyzed and the presence of F(ab)$_2$′ fragments was confirmed by 10% SDS-PAGE.

2.5. Ig protein determination

The protein concentration of each Ig pool was determined using the micro BCA protein assay (Pierce, Rockford, IL, USA). Pure pooled Ig samples from the original stocks were diluted 1/10 to 1/100 times in saline solution and then added 200 μL of the mixture of reagents A (bicinchoninic acid) and B (Cu^{2+}), according to the manufacturer's recommendations. Samples were incubated in duplicate at 37 °C for 30 min before measuring optical density (OD) at 570 nm. Each sample's protein concentration was determined by comparing its absorbance against a calibration curve obtained from 0 to 8 μg samples of a 2 mg/mL BSA standard diluted in PBS (see Table 2). The color complex was stabilized by adding 50 μL of 1N NaOH.

2.6. Immunohistochemistry techniques

2.6.1. Direct and indirect Dot blotting

In order to assure the isolation of Ig specifically raised against a particular pseudopeptide, direct and indirect immuno-dot assays were performed on each Ig isolation step. In brief, 5 μL aliquots of each Ig sample were spotted onto nitrocellulose membrane for direct Dot blotting (Bio-Rad Laboratories, Hercules, CA). For indirect Dot blotting, 5 μg of each 1513 pseudopeptide were first spotted before adding Ig samples. Membranes were blocked with 0.1% Tween-5% skimmed milk (w/v) in PBS for 1 h at room temperature. Indirect Dot blotting membranes were incubated with primary antibody (Ig pooled samples) overnight at 4 °C. Direct and Indirect Dot membranes were incubated with Horse Alkaline Phosphatase Anti-rabbit IgG (H + L) (Vector Laboratories, Inc. Burlingame, CA) diluted 1/1000 for 1 h at room temperature under constant shaking. Membranes were incubated with an activating solution (5 mM $MgCl_2$, 0.1 M NaCl, 0.1 M Tris–HCl, pH 9.5) for 40 min and immunostaining was detected using an BCIP/NBT solution (Promega, Madison, WI, USA)

2.6.2. ELISA tests

Enzyme-linked immunosorbent assays (ELISA) were performed for detecting antibody presence and measuring Ig pools' isotypes once being purified. Briefly, each ELISA microplate-well (Nunc, Inter, Med, Denmark) was coated with 100 μL of 0.005 μg/μL pseudopeptide as well as with *P. falciparum* lysate dissolved in bicarbonate buffer, pH 9.63. 100-μL samples of pure Ig pools diluted 1:100 were tested in duplicate after blocking wells with 3% skimmed milk in 0.05% PBS-Tween-20. Specific anti-tested compound activity was detected using a 1/1000 goat anti-rabbit IgG (H + L) peroxidase conjugate (Vector Laboratories, Inc. Burlingame, CA). A TMB developing solution (KLP, Gaithersburg, USA) was used as substrate. The reaction was stopped by adding 50 μL of 1 M H_3P0_4 per well. Results were expressed as OD values obtained at 450 nm.

2.6.3. Immunoblotting

P. falciparum-schizont lysate was dissolved in Laemmli's buffer, using β-mercaptoethanol as reducing agent and resolved on 10% SDS-polyacrylamide gels (Green and Kreier, 1978). The resolved proteins were electro-transferred to nitrocellulose membrane (Smythe et al., 1988). The antibody Ig pools or the rabbit sera were used as primary antibodies and were detected using goat anti-rabbit IgG (H + L) alkaline phosphatase conjugate (Vector Laboratories). A BCIP/NBT solution (Promega, Madison, WI, USA) was used as reaction substrate

2.6.4. Indirect immunofluorescence assay (IFA)

Synchronized-*P. falciparum* mature schizont-infected RBCs were fixed with methanol at −20 °C on multi-well slides (ICN, Pharmaceuticals Inc., Irvine, CA, USA). Wells were incubated with a 1/100 dilution of pre-immune and post-immune rabbit sera for 1 h at room temperature and a 1/1200 dilution of goat anti-rabbit IgG (H + L) isothiocyanate-fluorescein conjugate was added (Vector Laboratories, Inc. Burlingame, CA) to each well and let react for 1 h at room temperature. Slides were visualized under a fluorescence microscope (Olympus AXS 50, Tours, France).

2.7. In vitro malarial invasion inhibition by pseudopeptide-BSA conjugates and F(ab)$_2$′ antibody fragments

Antibodies were tested for their ability to inhibit *P. falciparum* (FCB-2 strain) invasion of human RBCs in *in vitro* assays. Ring-stage-iRBCs (>5% parasitemia) were synchronized using the sorbitol technique (Lambros and Vanderberg, 1979) and incubated in complete RPMI 1640 media supplemented with 25 mM HEPES buffer, 1 mg/mL hypoxanthine, 40 μg/mL gentamycin, 5 U/mL penicillin, 2 g/L glucose, 5% $NaHCO_3$ and 10% 0+ plasma. When parasites had reached the schizont stage, 96-well plates containing three antibody dilutions (1:2, 1:4 and 1:8) were seeded with cultured iRBCs and additional non-iRBCs for completing a final 100 μL volume per well at 1.5% hematocrit and 0.3% parasitemia. All antibodies were assessed in triplicate, being incubated for 18 h at 37 °C in 5% O_2, 5% CO_2, and 90% N_2. Cells were harvested after centrifugation and 50 μL supernatant were removed and replaced by 100 μL, 15 μg/mL hydroethidine (van der Heyde et al., 1995). The pellet was resuspended in 300 μL PBS following further incubation at 37 °C for 30 min and washes with PBS, then poured into polystyrene tubes and for quantifying parasitemia by flow cytometry using a FCAScan equipment (Becton Dickinson, San José, CA). The sequence of events was recorded and analyzed using Cell Quest software. An FSC x FL_2 profile was used for establishing an inclusion gate for non-iRBCs. Parasitized-RBCs were then quantified by quadrant analysis. Normal RBCs and parasitized RBCs in 15 μg/mL Ethylene glycol tetraacetic acid (EGTA) were used as controls. Invasion inhibition was calculated as being 100 × (% parasitemia in control − % parasitemia in test)/(% parasitemia in control).

2.8. Passive immunization of BALB/c mice with F(ab)$_2$′ induced against pseudopeptides and infection with Plasmodium yoelii 17XL malarial parasites

Murine parasite *P. yoelii* 17XL was thawed and subsequently grown *in vivo* by intraperitoneally infecting a first group of BALB/c mice with 1×10^6 iRBCs. A second group of mice was infected via tail vein inoculation. For *in vivo* parasite passages, iRBCs were collected in PBS-heparin, parasitized cells were quantified by microscopic analysis of thin smears of *P. yoelii*-parasitized RBCs and blood samples were diluted in PBS. The chloroquine resistant *P. falciparum* Colombian FCB-2 strain was used for immunohistochemistry assays (Espinal et al., 1982).

2.8.1. Standardization of Plasmodium yoelii infection kinetics in BALB/c mice

In order to establish a malarial *in vivo* infection in BALB/c mice (obtained from the *Universidad Nacional de Colombia* mouse-breeding facility), a cryo-preserved *P. yoelii* 17XL rodent malarial strain stored in 30% glycerol containing 100 UI/mL heparin RPMI medium was thawed and heated at 37 °C and subsequently washed with non-supplemented RPMI medium. The so obtained strain having a 80% viability, was centrifugated at 1500 rpm for 5 min as previously reported (Ramos-Avila et al., 2007; Spencer et al., 2008), the pellet containing about 1×10^7 infected red blood cells (iRBCs), was resuspended in 1 mL of RPMI and immediately used for intraperitoneally inoculating five BALB/c mice, each administrated with an average of 2×10^6 iRBCs. Parasitemia in all infected animals was monitored by Giemsa staining of blood-smear, evidencing that mice became parasitized by the second day post-infection and that parasitemia levels increased slowly until the animal died between 10 and 12 days after being infected. *P. yoelii* blood-stage life cycle did not developed synchronically during the 24 h following inoculation, as has been described elsewhere (Janse and Waters, 1995).

2.8.2. Passive immunization of BALB/c mice with F(ab)$_2$′ fragments and experimental murine malarial challenge

Groups of four 6-week-old BALB/c female mice were immunized with purified F(ab)$_2$′ Ig antibody fragments or saline solution (control group) on days −1, 0, 1 and 5 (being day 0 the day of *P. yoelii* 17XL infection), according to previously described protocols (Spencer et al., 1998; Lukasz et al., 2002). An infective dose of 5×10^4 infected RBCs (iRBCs) was established for the malarial experimental challenge. Parasitemia was monitored daily until day 15 by counting 1000 peripheral blood RBCs (healthy and infected) on a Giemsa-stained blood-smear, according to a protocol described elsewhere (Boyle et al., 1982; Majarian et al., 1984). The data so obtained were recorded in a database for later analysis. Serum was isolated from blood samples collected by retro-ocular puncture on days −1 and on the day animals were sacrificed

2.9. F(ab)$_2$′ structural elucidation by Circular Dichroism experiments

Circular Dichroism (CD) assays were performed at room temperature on nitrogen-flushed cells using a Jasco J-810 spectropolarimeter (Madrid, Spain). Spectra were recorded within a 190–250 nm wavelength interval using a 1-mm path length rectangular quartz cell. Each spectrum was obtained by averaging three scans taken at a scan rate of 20 nm/min with a 1-nm spectral band-width and corrected for baseline deviation using Jasco software. The CD profile of each F(ab)$_2$′ Ig molecule was obtained by analyzing 90 μg/mL protein preparations dissolved in (i) 50 mM PBS, pH 7.0, or (ii) 0–30% aqueous 2,2,2-trifluoroethanol (TFE) in a final volume of 500 mL. Results were expressed as mean residue ellipticity (θ), being the units degrees cm^2 dmol^{-1} according to the $(\theta) = \theta_\lambda/(100lcn)$ function where θ_λ corresponds the measured ellipticity, l the optical path length, c the peptide concentration and n the number of amino acid residues in the sequence.

3. Results

3.1. Rational pseudopeptide design and bioinformatics analysis

Five sequences were found by screening the Plasmodb database for *P. falciparum* MSP-1 orthologous sequences. Such sequences were located in the *P. berghei*, *P. chabaudi*, *P. knowlesi* H strain, *P. vivax* and *P. yoelii yoelii* 17XNL genomes. The multiple alignment between the sequences of peptide 1513 (MSP-1^{42-61}) and MSP-1 from *P. falciparum, P. vivax* and *P. yoelii* showed a 30% identity

between these sequences. The comparison between *P. falciparum* MSP-1$^{42–61}$ and its orthologous sequence in *P. yoelii* showed a 42.11% identity. Additionally, a 21.05% of high similarity, 21.05% of low similarity and a 15.79% of difference were found between both sequences. Regarding *P. falciparum* MSP-1$^{42–61}$ and its orthologous sequence in *P. vivax*, a 35% identity, 20% of high similarity, 15% of low similarity and a 30% of difference were found. In consequence, the orthologous sequence of *P. yoelii* presented the higher homology with *P. falciparum* MSP-1, as can be observed in Fig. 1A. Fig. 1B shows the identity and conservation values between each of the residue in the target sequences when analyzed by using the Jalview Java Alignment Editor. According to this analysis, a high conservation refers to conservation of the physical and chemical properties of each amino acid, being 11 the highest score and 3 the lowest value observed in this analysis. Amino acid positions having identities higher than 80% are shown shadowed in darker blue.

The genetics organization of *P. falciparum* MSP-1 allowed us to design a set of reduced amide pseudopeptides based on the sequence of peptide 1513 corresponding to the MSP-1$^{42–61}$ *N*-terminal sequence, as can be observed in Fig. 2A. Thus, based on the bioinformatics analysis, we decided to synthesize the 1513 native sequence and its five derived reduced amide pseudopeptides, all coupled to a BSA carrier, as indicated in the model displayed in Fig. 2B, according to the protocols described in Section 2. All pseudopeptide-BSA conjugates were analyzed and characterized by 7.5% SDS-PAGE (data not shown but available). All conjugates displayed similar electrophoretical profiles, having species with molecular weights higher than the relative molecular size of BSA (66–69 kDa), and all peptide or pseudopeptide conjugates displayed an average concentration of 100 μg/mL. Therefore, all of them were employed for immunizing rabbits and hence obtain antibody-enriched sera.

3.2. Antibody isolation and characterization

To eliminate antibodies directed against BSA, an absorption dose-dependent curve was established by treating all serum antibodies with BSA concentrations ranging between 20 and 250 mg. The later concentration was proven to be effective for completely removing antibodies reactive against BSA, as shown in Fig. 3A.

After removing anti-BSA antibodies, all rabbit serum samples obtained after the sixth immunization were analyzed by ELISA and Western blot to verify each pseudopeptide's antigenicity against its corresponding 1513 parent sequence and correlate such antigenicity with its antibody titers. In agreement with the cut-off point observed in Fig. 3B, antibody titers raised against 1513 ranged from 1:640 to 1:2560, as can be observed in Table 1, which demonstrates specific antigenic properties of each pseudopeptide conjugate. The antibody titers induced by each of the five pseudopeptides were as follows: Ig-α-ψ-437 1:10240, Ig-α-ψ-439 1:10240, Ig-α-ψ-440 1:5120, Ig-α-ψ-441 1:2560 and Ig-α-ψ-442 1:1280. Furthermore, Indirect Immunofluorescence Analyses (IFA) demonstrated the immunogenic properties of each designed molecule since the MSP-1 present in mature-schizonts on infected red blood cells (iRBCs) was clearly recognized by Igs from animals being immunized with pseudopeptides, probable due to recognition of the MSP-1 natively expressed by the malaria parasite, as indicated by the immunofluo-

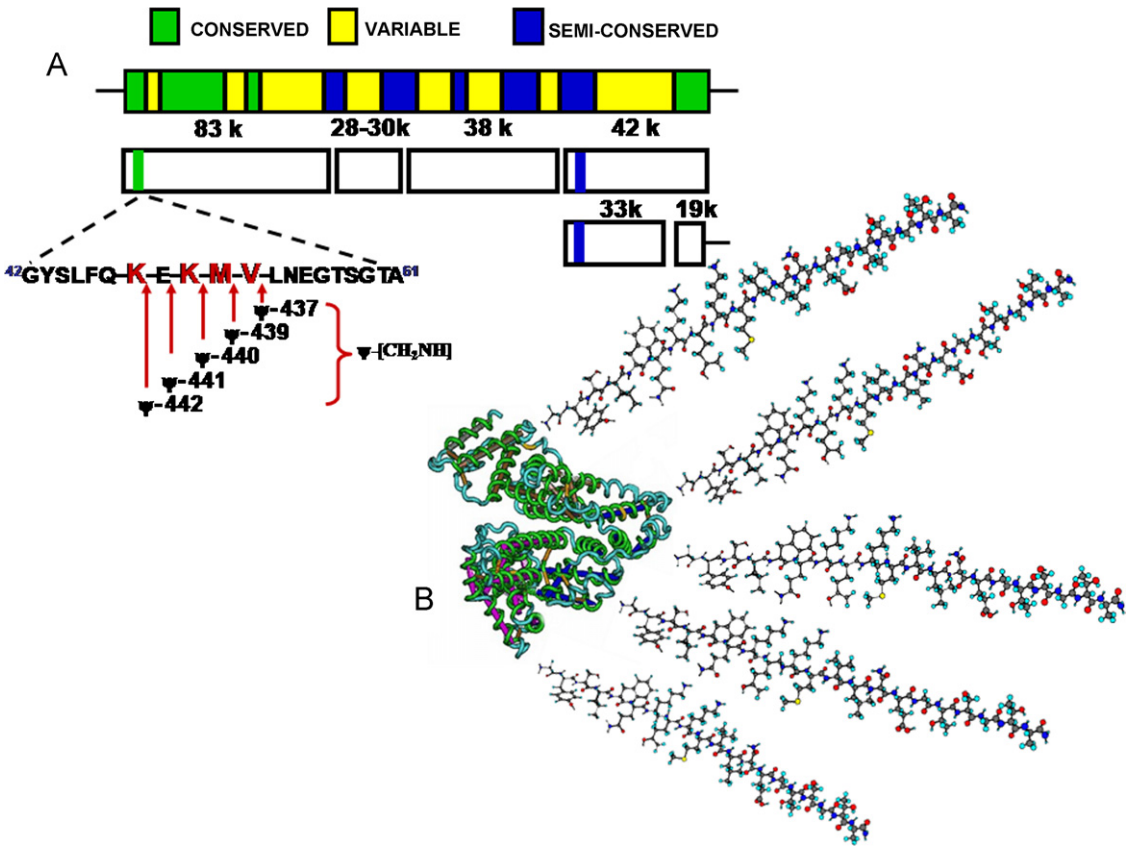

Fig. 2. Experimental design of the MSP-1$^{42–61}$ derived pseudopeptides. (A) Schematic representation of the *Plasmodium falciparum* merozoite surface protein-1 in which the primary structure of peptide 1513 as well as its genetic organization is shown. Conserved domains are colored in green, non-repetitive dimorphic domains blocks in blue, and blocks representing highly genetic polymorphism regions in yellow. The 1513 high binding motif to RBC ^{48}K-KMV^{52} is the basis for all reduced amide pseudopeptide analog design. (B) Structural simulation of the 1513 peptide and its pseudopeptide analogs coupled to BSA through a glutaraldehyde cross-linker. (For interpretation of the references to color in this figure legend, the reader is referred to the web version of the article.)

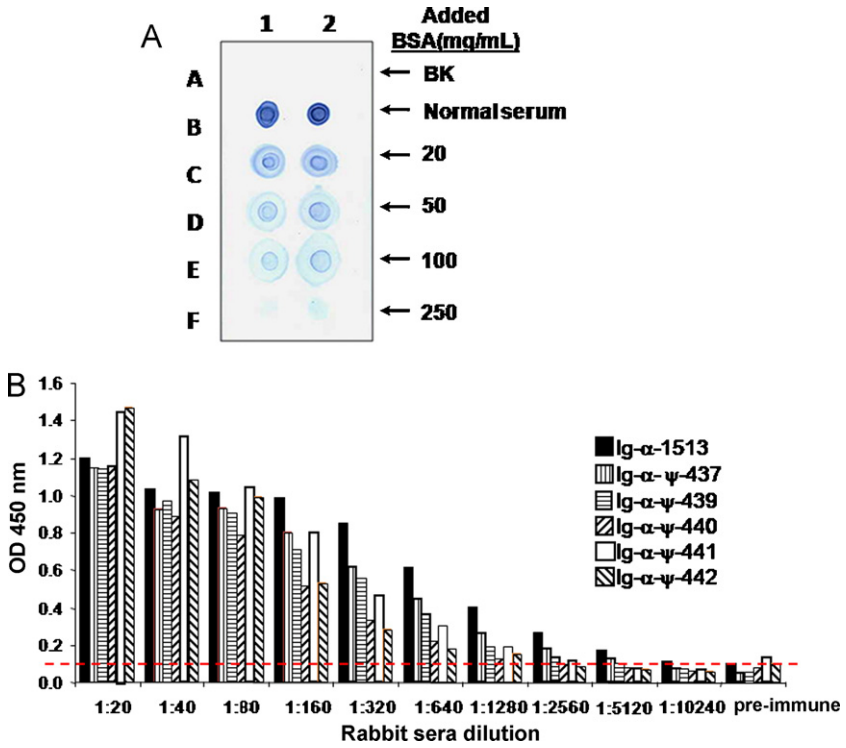

Fig. 3. Antigenicity of partially purified rabbit antibodies. (A) Direct dot showing the efficient absorption of anti-BSA specific antibodies by treating serum samples with increasing amounts of BSA. (B) Antibody titers induced against peptide 1513 and its derived pseudopeptide analogs. Antibody titers were determined as the highest dilution greater than the cut-off value, represented by dotted line. The mean OD_{450} value of control sera ± 3 standard deviations (SD) corresponded to the titer of the sample.

Table 1
Characterization of immunoglobulin and F(ab)$_2$′ purified molecules.

Serum name	Antibody titer (Ig to BSA-absorbed) α-1513/itself		Serum protein	Ig-Ammonium sulfate protein precipitated	Ig-pool from Anionic exchange chromatography		F(ab)$_2$′
			(μg/mL)	(μg/mL)	(μg/mL)	vol (mL)	(μg/mL)
α-1513	1:2560	1:2560	5.99	15.98	41.28	9.00	102.00
α-ψ-437	1:2560	1:10240	6.11	13.90	40.09	16.00	66.60
α-ψ-439	1:1280	1:10240	7.05	18.46	66.86	54.00	137.00
α-ψ-440	1:640	1:5120	5.75	11.64	47.87	46.00	57.40
α-ψ-441	1:1280	1:2560	7.99	13.96	76.95	51.00	97.60
α-ψ-442	1:640	1:1280	5.61	11.76	72.89	29.00	80.00

rescence studies. As clearly observed in shown in Fig. 4, antibodies raised in animals being inoculated only with BSA (assay control) did not recognize the malaria parasite (Fig. 4A and B), while antibodies raised in animals being immunized with the pseudopeptides designed by us specifically recognized the malaria parasite (Fig. 4D and F). On the contrary, antibodies obtained from the pre-immune serum samples of the same animals clearly showed a lack of reactivity against the parasite (Fig. 4C and E).

3.3. Antibody mapping for specific 1513's sequence recognition

With the aim of precisely establishing the specific reactivity of each pseudopeptide-induced antibody on the native 1513 peptide sequence, a set of 1513 C- and *N*-terminally truncated sequences were synthesized and characterized as shown in Table 2. A subsequent ELISA test showed that antibodies to the 1513 native sequence were notoriously poly-specific since they recognized the complete primary structure of the peptide as shown in Fig. 5A. Remarkably, antibodies induced by any of the 1513 pseudopeptides were specifically directed to the *C*-terminal portion of the MSP-$1^{42–61}$ 1513 peptide, being analogs 9491, 9493 and 9495 the most strongly recognized peptides, while those antibodies induced by the non-modified 1513 peptide polyspecifically recognize the entire sequence. Antibodies induced by each pseudopeptide were analyzed for their specificity as determined by indirect dot as show in Fig. 6A. According to our results, the consensus sequence that better represents this possible B-epitope is: ^{51}MVLNEGTSGTA^{61} or MSP-$1^{51–61}$. In all performed antigenicity tests, Igs present in sera samples poorly recognized the peptide coded 1585 (MSP-$1^{1282–1301}$) as a non-relevant sequence. This

Table 2
Characterization of native MSP-$1^{42–61}$ (1513 peptide) and its truncated analogs.

Peptide	Sequence	MW (Da)
1513	GYSLFQKEKMVLNEGTSGTA	2160.6
9490	GYSLFQKEKMV	1329.6
9492	GYSLFQKKKM	1230.5
9494	GYSLFQKEK	1099.3
9496	GYSLFQKE	971.1
9498	GYSLFQK	842.0
9500	GYSLFQ	713.8
9491	LNEGTSGTA	849.0
9493	VLNEGTSGTA	948.1
9495	MVLNEGTSGTA	1079.3
9497	KMVLNEGTSGTA	1207.5
9499	KKMVLNEGTSGTA	1336.6
9501	KEKMVLNEGTSGTA	1464.8

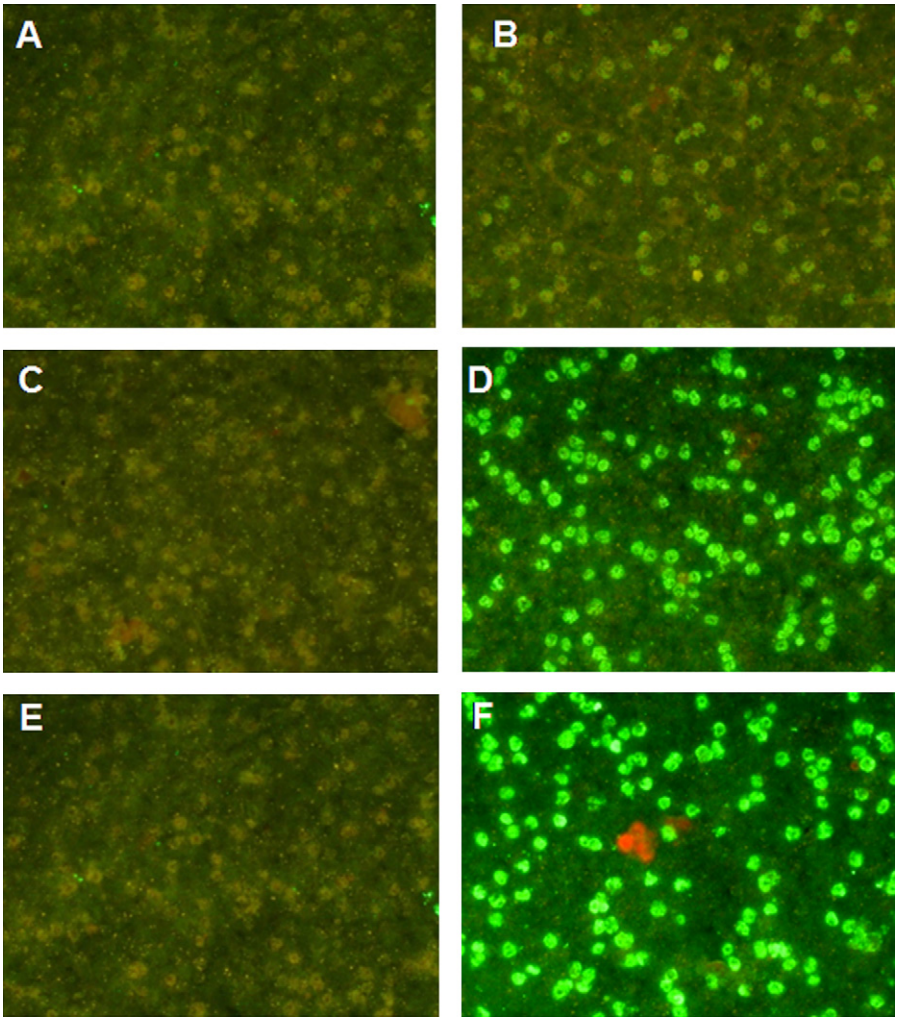

Fig. 4. Specific recognition of *Plasmodium falciparum* native proteins by rabbit Ig directed to 1513 pseudopeptides. Immunofluorescence patterns of pre-immune sera (left-hand panels) and post-sixth immunization sera (right-hand panels) specifically recognized *Plasmodium falciparum* mature schizonts. Experiment controls immunized with BSA (A and B). Rabbit immunized with ψ-439 (Met-Val)-BSA conjugate (C and D). Rabbit immunized with ψ-440 (Lys-Met)-BSA conjugate (E and F).

later sequence is derived from the *C*-terminal portion of MSP-1, its primary structure being ^{1282}EVLYLKPLAGVYRSLKKQLE^{1301}. Sera reactivity against 1585 was comparable to that observed against BSA, as shown in Fig. 5. PBS was used as blank.

After being extensively characterized, all Ig samples were subjected to a classical double-step procedure consisting in ammonium sulfate saturation followed by a weak Anionic Exchange Chromatography (AEC), as described in Methods. As observed in Fig. 6B, mono-specific antibodies induced by the 1513 pseudopeptides, obtained by successively increasing the buffer's ionic strength, specifically cross-reacted with *P. falciparum* protein fragments in a Western blot analysis at molecular relative masses of 195 kDa, 113 kDa, 83 kDa, 47–52 kDa and 31–36 kDa. This recognition pattern is consistent with previously reported information regarding MSP-1 processing (Holder et al., 1992; Kauth et al., 2003). Fractions that were reactive by Western blot were then pooled and analyzed in a second round of experiments by different immunohistochemistry techniques to confirm these antibodies' specificity. As can be observed in Fig. 6C, the electrophoretical pattern of Ig polled samples recognized bands having relative molecular mobilities of 195–200 kDa, 152 kDa, 83 kDa, 73 kDa and 52–47 kDa, which are in agreement with the molecular weights of the entire MSP-1 molecule and its processed products reported in the literature (Holder et al., 1992; Kauth et al., 2003).

Additionally, each immunoglobulin's electrophoretical profile was determined by 10% SDS-PAGE under mild reducing conditions. As shown in Fig. 7A, the entire Ig molecule had a relative mobility of 150 kDa, $F(ab)_2'$ Ig fragments were detected at 95–100 kDa, heavy chains at 47.5 kDa and 62 kDa, Fab at 50 kDa, while light chains and Fc-Ig portions are observed at 25 kDa and 32.5 kDa, respectively.

Once being homogenously purified, each Ig reactive pooled fraction was subjected to a papain Ig-digestion as previously reported (Gregory et al., 2003). This procedure was successfully performed in an over-night assay as can be seen in Fig. 7B, since bands corresponding to the partially digested Ig molecules having a molecular relative mobility between 121 kDa and 212 kDa were clearly observed, as well as a strong band of about 100 kDa to 96 kDa corresponding to $F(ab)_2'$-Ig fragments, a band of about 50 kDa corresponding to the Fc portion and a faster band migrating lower than 36.5 kDa, which seems to be consistent with the 23 kDa molecular weight of papain (lane 4d).

Affinity purification of the $F(ab)_2'$ fragments was carried out using Protein-A sepharose resin. $F(ab)_2'$-Ig fragment isolation was analyzed by SDS-PAGE as displayed in Fig. 7C where a strong band having a relative mobility about between 100 kDa to 96 kDa is observed. As shown in Table 1, all pseudopeptide-induced $F(ab)_2'$-Ig fragments were obtained in sufficiently large amounts as to perform functional *in vitro* and *in vivo* experiments.

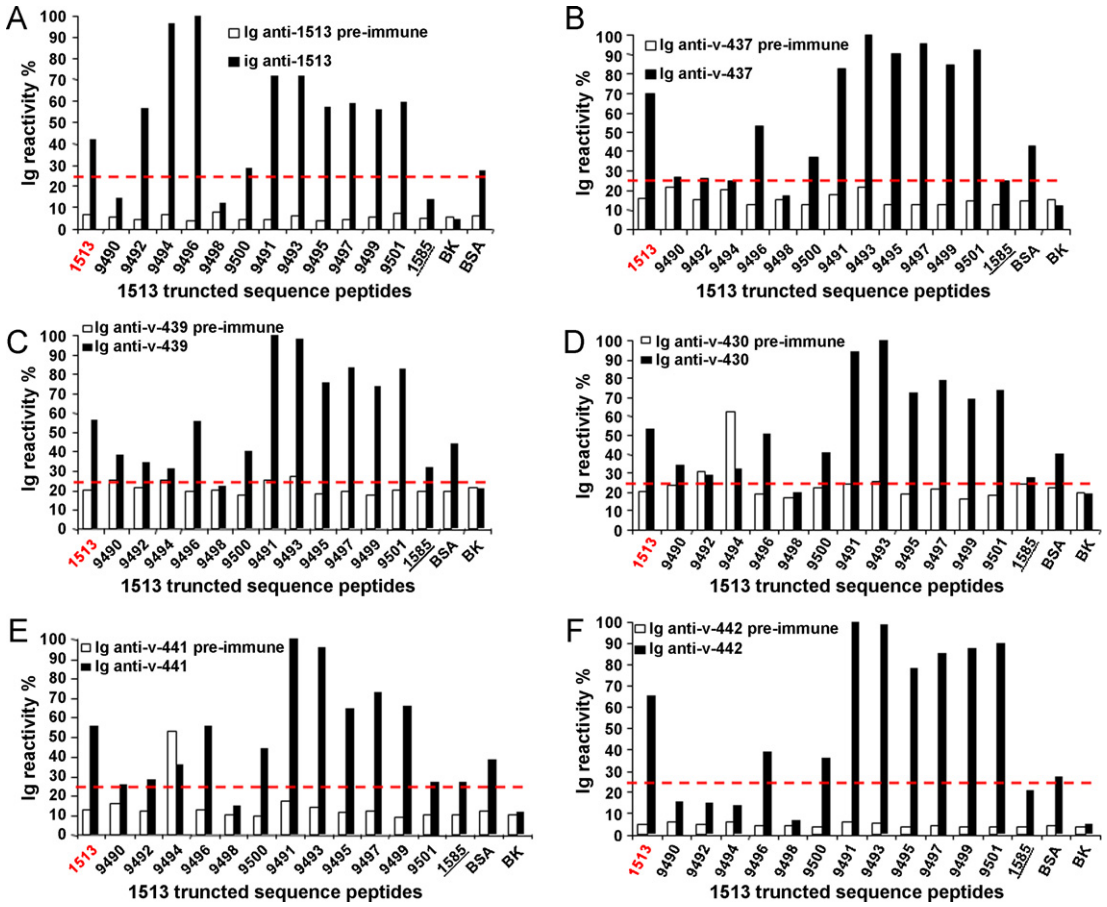

Fig. 5. Mapping of 1513-pseudopeptide induced antibodies by competition ELISA. Ig reactivity % in all cases was normalized by selecting the highest optical density at 450 nm as the 100% reactivity. The threshold was arbitrarily established as 25% (dotted red lines). (A) Reactivity of polyclonal antibodies induced by the entire native peptide 1513 sequence (in red) (MSP-1^{42-61}). (B) Reactivity of polyclonal antibodies induced by the pseudopeptide ψ-437 (Val-Leu). (C) Reactivity of polyclonal antibodies induced by the pseudopeptide ψ-439 (Met-Val). (D) Reactivity of polyclonal antibodies induced by the pseudopeptide ψ-440 (Lys-Met). (E) Reactivity of polyclonal antibodies induced by the pseudopeptide ψ-441 (Glu-Lys). (F) Reactivity of polyclonal antibodies induced by the pseudopeptide ψ-442 (Lys-Glu). In all cases peptide 1585 was employed as a non-relevant sequence, BSA as control and PBS as blank. (For interpretation of the references to color in this figure legend, the reader is referred to the web version of the article.)

3.4. Pseudopeptide-BSA conjugates and their derived F(ab)$_2'$ antibody-fragments displays in vitro neutralizing activity

Pseudopeptide-BSA conjugates inhibited the process only at a 0.5 mg/mL concentration while their induced specific antibodies do it at very low concentrations lower than 60 μg/mL (Fig. 8). On the other hand most of the obtained specific-Ig pooled purified fractions inhibited *P. falciparum* human RBC-invasion at some degree. The Ig pools used for passive immunization experiments inhibited the parasite invasion to RBCs by approximately 53% at an Ig concentration of 0.12 μg/mL, while Ig fraction pools 3 (F(ab)$_2'$ to ψ-437), 15 (F(ab)$_2'$ to ψ-441), 24 (F(ab)$_2'$ to ψ-439), 32 (F(ab)$_2'$ to ψ-439), 11 (F(ab)$_2'$ to ψ-440) and 16 (F(ab)$_2'$ to ψ-442) inhibited invasion by 84%, 87%, 27%, 44%, 68% and 66%, respectively at concentrations lower than 100 μg/mL. Ig pool 19 (F(ab)$_2'$ to ψ-442) reached a maximum inhibition of 60% at an Ig concentration of 0.06 μg/mL; however, only Ig pools 24 (F(ab)$_2'$ to ψ-439), 32 (F(ab)$_2'$ to ψ-439), 15 (F(ab)$_2'$ to ψ-441) and 19 (F(ab)$_2'$ to ψ-442) displayed a dose-dependent inhibition pattern. Reactivity of purified pooled F(ab)2′-Ig fragments displayed in Fig. 8 were grouped as follows: F(ab)$_2'$ to ψ-437 (pools 2–3), F(ab)$_2'$ to ψ-439 (pools 4–7), F(ab)$_2'$ to ψ-440 (pools 9–11), F(ab)$_2'$ to ψ-441 (pools 13–15), F(ab)$_2'$ to ψ-442 (pools 16–20), F(ab)$_2'$ to nm-1513 (pools 35–37).

3.5. Establishing a Plasmodium yoelii in vivo infection model

Following the intravenous inoculation of female BALB/c mice with a lethal dose (2×10^6 iRBCs) of the *Plasmodium yoelii* 17XL strain, animals were followed-up over a fixed time period of 10 days in order to evaluate the appearance and establishment of parasitemia. Twenty-four hours after being infected, most animals reached a mean 0.2% parasitemia, as evidenced by the presence of immature *Plasmodium* forms such as ring-stages in the blood samples collected from all mice. Parasitemia progressed during the first five days of post infection, allowing the appearance of different parasite stages such as rings, trophozoites and immature schizonts. From day six on, the malarial infection had become asynchronic. All animals had reached a 30.0% level of parasitemia by day six, bearing all the aforementioned forms in their blood plus mature schizonts and free merozoites. Therefore, after successfully infecting BALB/c mice, freshly obtained *Plasmodium yoelii* inoculums were used for passive immunization experiments by *in vivo* passages. In consequence, a delay in parasitemia onset after day six due to any antimalarial treatment can be considered as relevant. As previously reported by others, a successful *Plasmodium yoelii* 17XL infection of BALB/c mice is normally achieved by intravenously injecting 5×10^4 iRBCs, reaching a 20% of parasitemia at day five and a 50% of parasitemia at day seven (Ramos-Avila et al., 2007).

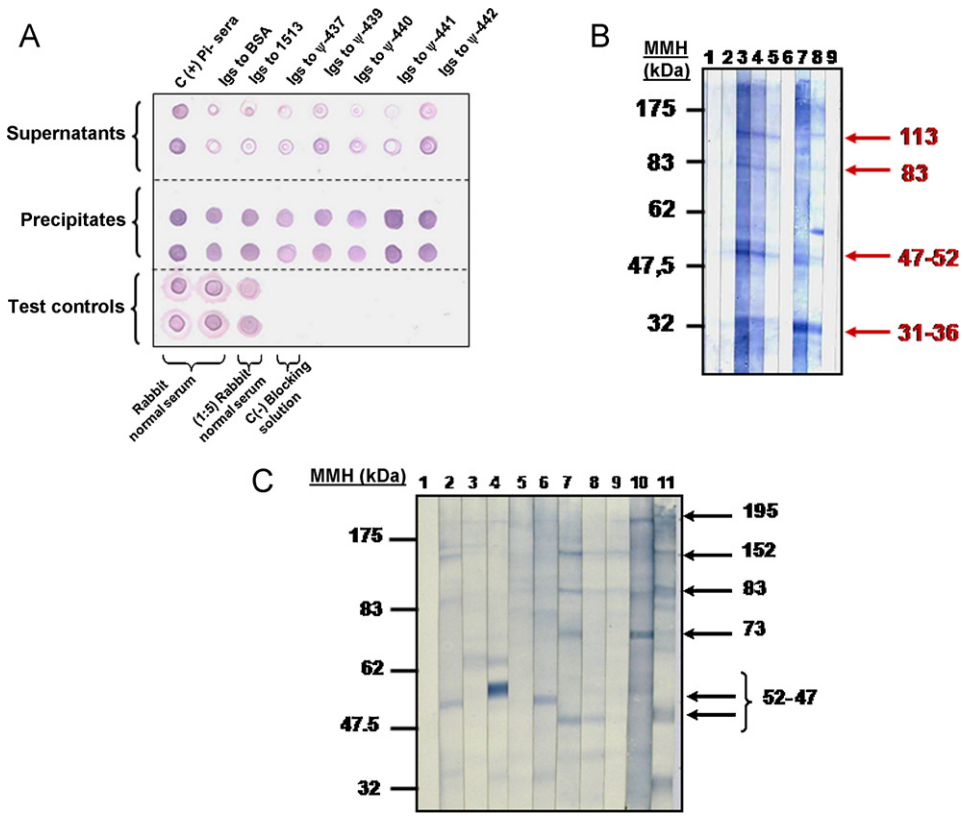

Fig. 6. Reactivity of 1513-pseudopeptides partially purified and totally purified antibodies after ammonium sulfate treatment. (A) Direct Dot blotting was used for detecting Ig reactivity of precipitates and supernatants following precipitation with ammonium sulfate. Reactivity of the Ig present in the supernatants are shown in the upper side of the figure, the reactivity of the Ig isolated in the pellets are displayed in middle panel of the figure, while the lower panel shows the reactivity of the positive and negative controls. (B) Western blot analysis of *Plasmodium falciparum* surface proteins with 1513-pseudopeptide antibodies purified by Anionic Exchange Chromatography. Lanes 1–9 are chromatography the Ig reactive fractions 12, 13, 14, 15, 17, 20 (eluted with 10 mM Tris–HCl, pH 8.3 + 100 mM NaCl), 38, 39 and 40 (eluted with 10 mM Tris–HCl, pH 8,3 + 500 mM NaCl). (C) Reactivity of Anionic Exchange Chromatography pooled fractions containing purified Ig, as assessed by Western blot analysis against *Plasmodium falciparum* surface proteins. Lane 1 is the negative control (blocking solution), lane 2 is a pool of fractions 14–18 (Ig against the native 1513 parent sequence), lane is 3 a pool of fractions 38–39 (Ig against the ψ-437 pseudopeptide), lane 4 is a pool of fractions 14–18 plus 20–21 (Ig against the ψ-439 pseudopeptide), lane 5 is a pool of fractions 39–41 (Ig against the ψ-439 pseudopeptide), lane 6 is a pool of fractions 12–14 (Ig against the ψ-440 pseudopeptide), lane 7 is a pool of fractions 39–42 (Ig against the ψ-440 pseudopeptide), lane 8 is a pool of fractions 11–16 (Ig against the ψ-441 pseudopeptide), lane 9 is a pool of fractions 36–40 (Ig against the ψ-441 pseudopeptide), lane 10 is a pool of fractions 14–16 (Ig against the ψ-442 pseudopeptide) and lane 11 is a pool of fractions 39–41 (Ig against the ψ-442 pseudopeptide).

3.6. Passive immunization experiments with defined $F(ab)_2'$-Ig fragments induced against 1513 pseudopeptides

Based on the data showing that $F(ab)_2'$-Ig fragments specifically directed against 1513-pseudopeptides possess the ability of inhibiting *in vitro* invasion of RBCs by a *P. falciparum* strain, *in vivo* assays were conducted in BALB/c mice. According to the growth kinetics of *Plasmodium yoelii* described above, the BALB/c mouse animal model was suitable for malarial infection experiments. Animals being infected with 5×10^4 iRBCs presented an average $0.5 \pm 0.3\%$, $22 \pm 15\%$ and $32 \pm 2\%$ parasitemia on days 6, 8 and 11. Mice in the control group managed a parasitemia infection average around 40% (Fig. 9) and normally did not survive beyond day 8, all mice belonging to the control group dye between the 3rd and 8th day of the experiment. In contrast, all mice's groups passively transferred managed higher parasitemia percentages, even twice than the control group as it can be observed in the same figure. The passive immunization of mice with $F(ab)_2'$ induced by pseudopeptides ψ-439 (Met^{51}-Val^{52}), ψ-440 (Lys^{50}-Met^{51}) and ψ-442 (Lys^{48}-Glu^{49}) delayed the onset of parasitemia while those $F(ab)_2'$ induced by ψ-437 (Val^{52}-Leu^{53}) and ψ-441 (Glu^{49}-Lys^{50}) did not confer a protective effect but animals managed very high parasitemia levels regarding the control group in which mature schizonts, rings and throphozoite forms of the malaria parasite can be clearly observed (Fig. 9C). Remarkably, an animal passively transferred with $F(ab)_2'$ induced against the ψ-440 (Lys^{50}-Met^{51}) isoster bond pseudopeptide, became fully protected and was able of rapidly clearing out malaria parasites from its blood stream. Under microscopic analysis, a blood smear taken from this protected animal presented some few asynchronic parasitic forms of *P. falciparum*, but none of them were able to invade any circulating RBCs (Fig. 9D). All animals belonging to the control group being injected with saline solution developed detectable parasitemia by day three and all died before day seven. As can be observed in Fig. 9B showing the survival profile of group 5, which was passively immunized $F(ab)_2'$ induced by the ψ-440 (Lys^{50}-Met^{51}) isoster bond pseudopeptide, this group controlled better the malarial infection caused by *Plasmodium yoelii* while groups immunized with $F(ab)_2'$ induced by the ψ-439 (Met^{51}-Val^{52}) and ψ-442 (Lys^{48}-Glu^{49}) isoster pseudopeptides partially controlled the infection by displaying a delay in parasitemia onset. Mice belonging to group 1, which were transferred with $F(ab)_2'$ to the native 1513 sequence, became rapidly infected and were not able to control malarial infection over the course of the study.

3.7. Secondary structure pattern of $F(ab)_2'$-Ig fragments

As can be observed in Fig. 9, all $F(ab)_2'$-Ig fragments tended to display strong classical β-strand profiles in CD experiments, displaying a characteristic molar ellipticity minimum at 220 nm, but were more clearly shown by $F(ab)_2'$-Ig fragments induced by

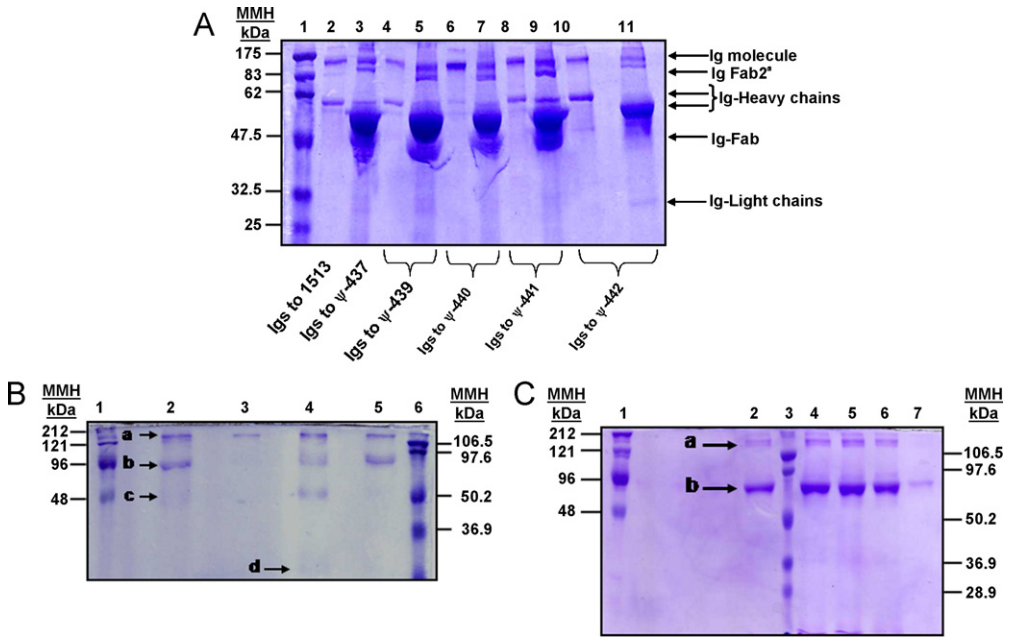

Fig. 7. (A) Ig electrophoretical characterization and F(ab)$_2$′ fractionation. A. Electrophoretical mobility profile of 1513 pseudopeptide-induced Ig resolved by 10% SDS-PAGE under mild reducing conditions after ammonium sulfate treatment. (B) Papain Ig digestion, *a* represents the entire Ig molecule, *b* represents the Ig-F(ab)2′, *c* shows Ig-heavy chains and *d* is the remaining papain. C. Ig-F(ab)$_2$′ to ψ-440 purified by affinity chromatography, lanes 2–7 for some eluted fractions. *a* represents the entire Ig molecule, *b* represents the Ig-F(ab)2. MWM for molecular weight markers. Assigned pairs, represent electrophoretical mobility of proteins present in supernatant, first lane and precipitate in the second lane.

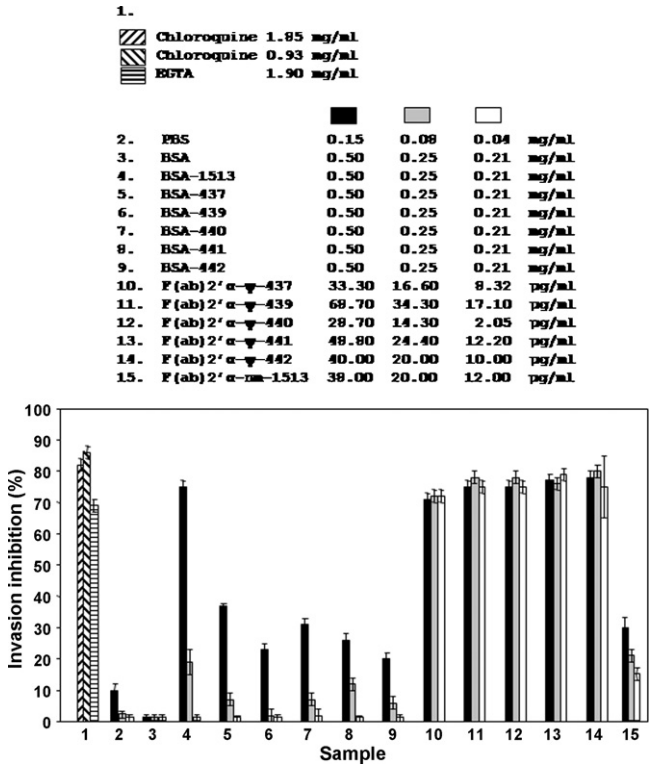

Fig. 8. *In vitro* neutralizing properties of 1513-BSA conjugates and their induced F(ab)$_2$′ fragments. F(ab)$_2$′ fragments possess neutralizing properties against *Plasmodium falciparum* invasion of RBCs. Samples 2–9 are all BSA-pseudopeptide conjugates. Samples 10–14 are the pooled purified F(ab)$_2$′ induced by pseudopeptides ψ-437, ψ-439, ψ-440, ψ-441, ψ-442, respectively and sample 15 the pooled purified F(ab)$_2$′ induced by the non-modified 1513 peptide.

pseudopeptides ψ-439 (Met^{51}-Val^{52}) and ψ-440 (Lys^{50}-Met^{51}), as indicated by green and light blue lines, respectively, in Fig. 10.

According to the analysis of deconvoluted CD data, the majority of F(ab)$_2$′ fragments consistently displayed β-strand shaped structures. Interestingly, those fragments that were not associated to any protective effect in the *in vivo* experiments possessed different secondary structure profiles, such as in the case of the F(ab)$_2$′ fragment induced against ψ-442 (Lys-Glu), which presented a low percentage of α-helical features characterized by the presence of two minima at 208 nm and 222 nm, respectively. These data are in agreement with previously reported literature (Kaufmann et al., 2006).

In order to obtain a closer interpretation of each secondary structure profile, all data were submitted to deconvolution by using the *Continll* program. The content of secondary structure elements is shown in Fig. 10. As can be observed, F(ab)$_2$′ induced against the parental peptide 1513 displays a high α-helical content of about 65.0% and 13.6% of β-strand features. Similarly, the F(ab)$_2$′ fragment induced against ψ-437, having a peptide bond replacement between the Val^{52}-Leu^{53} pair, shows a 39.1% of β-strand content and a 21.0% of turn features. The F(ab)$_2$′ fragment induced against ψ-439, which was modified between Met^{51}-Val^{52}, shows a 72.2% of β-strand content and 15.0% of turn features. The F(ab)$_2$′ fragment against ψ-440, modified between Lys^{50}-Met^{51}, shows an 85.2% of β-strand content and 10.6% of turn features. The F(ab)$_2$′ fragment induced against ψ-441, modified between Glu^{49}-Lys^{50}, shows a 15% of α-helical content, 35.2% of β-strand content and 22.8% of turn features. Finally, the F(ab)$_2$′ fragment induced against ψ-442, modified between Lys^{48}-Glu^{49}, displays a 75.0% of α-helical and 10.7% of β-strand content.

4. Discussion

Malaria is a transmissible disease that has become a serious worldwide public health problem due to the rapid spread and increased virulence of *Plasmodium* species. Despite global efforts to improve malaria control strategies, the disease is gaining ground

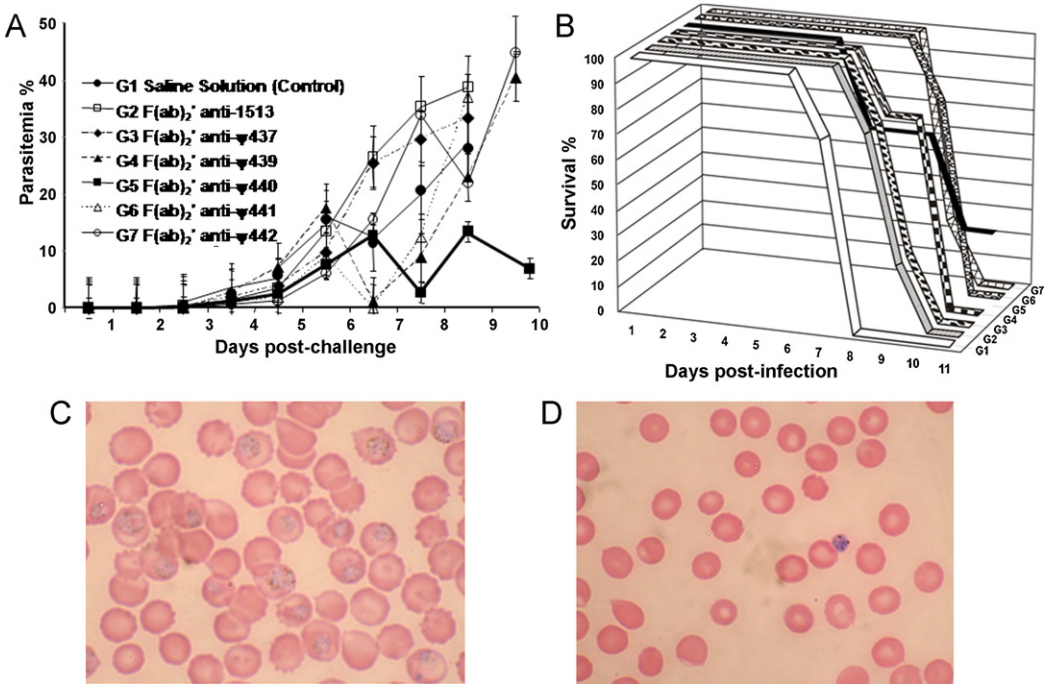

Fig. 9. Course of parasitemia in BALB/c mice inoculated with different doses of *P. yoelii*-infected RBCs. (A) Infection dose: 5×10^4 iRBCs. (B) Infection dose: 25,000 iRBCs. Each line represents the mean parasitemia of each animal group with its corresponding SD. (C) Parasitized mouse RBCs. D. Mouse 18 protected against malaria by passive transfer of F(ab)$_2'$ fragments induced against pseudopeptide ψ-440 (Lys^{50}-Met^{51}) was able to completely clear out malaria parasites.

and is day by day causing a larger number of cases and deaths. The influence of global warming, the increasing resistance of transmission vectors to insecticides and of parasites to antimalarial drugs, are further increasing the burden on public health systems and countries' economies. Thus, finding a potent malaria vaccine against this lethal disease is an urgent world need. A variety of merozoite surface antigens have been classically regarded as candidate targets for vaccine development. *Plasmodium* sporozoite molecules have been also evaluated in the same context, but so far a fully protective vaccine against this deadly disease has not been obtained.

By comparing the sequence of *P. falciparum* MSP-1$^{42–61}$ peptide with its orthologous in *P. yoelii*, allowed us to propose a site-directed pseudopeptide design. Thus, based on the bioinformatics analysis, we decided to synthesize and coupled the 1513 native sequence and its five reduced amide derived pseudopeptide analogs to BSA as carrier for *in vivo* experiments. All conjugates displayed a similar electrophoretical mobility pattern, all displaying species with relative molecular weights between 100 kDa to 175 kDa, higher than the 66–69 kDa relative molecular size of BSA. Anti-pseudopeptide specific antibodies were obtained by immunizing rabbits with each pseudopeptide and treating serum samples with BSA, which has been proven effectively for removing all reactivity against BSA. Antibody titers against the MSP-1$^{42–61}$ native sequence ranged between 1:640 and 1:2560, while as expected, specific antibody titers against each 1513 pseudopeptide analog were higher ranging between 1:1280 and 1:10240.

Immunogenicity tests demonstrated that antibodies directed against the 1513 native sequence polyspecifically recognized the whole primary structure of the MSP-1$^{42–61}$ fragment, whereas

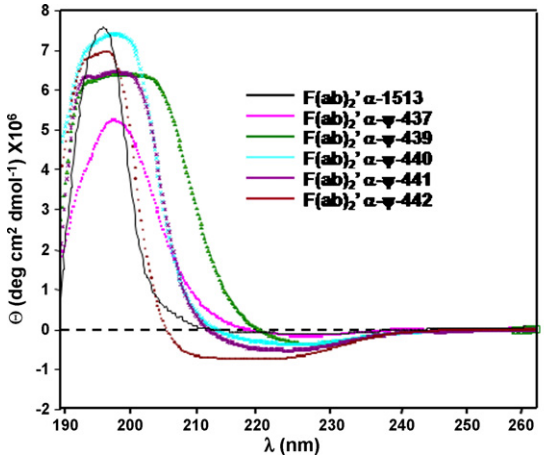

Data deconvolution with CONTINLL
Secondary structure element content

F(ab)$_2$'	H(r)	H(d)	S(r)	S(d)	Turn	Unrd
α-1513	**0.650**	0.034	0.037	0.136	0.113	0.030
α-ψ-437	0.092	0.034	**0.391**	**0.142**	**0.210**	**0.131**
α-ψ-439	0.035	0.043	**0.722**	0.010	**0.150**	0.040
α-ψ-440	0.010	0.014	**0.852**	0.006	**0.106**	0.012
α-ψ-441	**0.150**	0.034	**0.352**	**0.142**	**0.228**	0.094
α-ψ-442	**0.750**	0.034	**0.107**	0.020	0.058	0.031

Fig. 10. Secondary structure profile of F(ab)$_2'$-Ig fragments. Circular Dichroism experiments were performed to analyze possible secondary patterns present in 1513-pseudopeptides. The figure shows CD profiles of F(ab)$_2'$-α-1513 (black line), F(ab)$_2'$-α-ψ-437 (pink line), F(ab)$_2'$-α-ψ-439 (green line), F(ab)$_2'$-α-ψ-440 (light blue line), F(ab)$_2'$-α-ψ-441 (purple line) and F(ab)$_2'$-α-ψ-442 fragments (brown line). CD deconvoluted data is shown in right chart. (For interpretation of the references to color in this figure legend, the reader is referred to the web version of the article.)

antibodies induced by the site-directed designed 1513 pseudopeptides were specifically directed to the C-terminal portion of the MSP-1^{42-61} 1513 peptide sequence. Such results demonstrate the versatility of the approach followed in this study for revealing possible B-epitopes within a given sequence. Ig mapping indicated that the sequence that better represents such B-epitope is: ^{51}MVLNEGTSGTA^{61} or MSP-1^{51-61}, which is located between the highly conserved block 1 and the dimorphic block 2 of MSP-1 (Avila et al., 2000). As previously published by us, NMR experiments demonstrated that the *C*-terminal portion of all modified sequences of this protein fragment, display extended conformations which reflects a high energy content of the molecule enabling a better fit to a potential receptor on a cell surface (Lozano et al., 1998).

The recognition patterns of anti-pseudopeptide Ig is consistent with the proteolytic processing of MSP-1 that results in cleavage fragments with relative molecular masses of 195 kDa, 113 kDa, 83 kDa, 72–73 kDa, 47–52 kDa and 31–36 kDa, as has been widely reported in the literature, and all of which contain the MSP-1^{42-61} sequence (Holder et al., 1992; Jouin et al., 2001; Miller et al., 1993). Thus, antibodies raised against site-directed designed pseudopeptides were able to specifically recognize the target molecule and have revealed the presence of a potential new B-epitope on the protein.

Papain digestion of the anti-pseudopeptide Ig chains was successfully performed, as evidenced by the strong band of about 96 kDa obtained by SDS-PAGE and Western blot analyses, which agrees the molecular weight expected for $F(ab)_2'$-Ig fragments. Besides, protein concentration of all 1513-pseudopeptide-induced $F(ab)_2'$-Ig fragments was in sufficient amount to perform functional *in vitro* and *in vivo* assays.

As previously assessed, $F(ab)_2'$-Ig fragments specifically directed against 1513-pseudopeptides inhibited the *in vitro* the invasion of RBCs by a *P. falciparum* strain, being the basis for *in vivo* experiments in BALB/c mice. Thus, immunized BALB/c mice challenged with a lethal dose of a *Plasmodium yoelii* 17XL strain, showed a differential ability for controlling malarial infection. Mice being passively immunized with $F(ab)_2'$ induced by pseudopeptides ψ-439 (Met^{51}-Val^{52}), ψ-440 (Lys^{50}-Met^{51}) and ψ-442 (Lys^{48}-Glu^{49}) delayed onset of parasitemia, while those $F(ab)_2'$ induced by ψ-437 (Val^{52}-Leu^{53}) and ψ-441 (Glu^{49}-Lys^{50}) had no protective effect, as evidenced by the development of parasitemia levels comparable to the ones of the control group. Remarkably, some of the animals that were passively transferred with $F(ab)_2'$ induced by the ψ-440 (Lys^{50}-Met^{51}) isoster bond pseudopeptide became fully protected and were able to clear out malaria parasites from their blood streams, remaining parasite-free for a long period of time. By contrast, the group of animals that was transferred with $F(ab)_2'$ directed to the native 1513 sequence and those being injected with saline solution, became rapidly infected and were not able to control the malarial infection during the course of the study.

We found an evident trend for $F(ab)_2'$-Ig fragments associated to a delayed onset of parasitemia to display a strong β-strand classical profiles as judged by CD experiments, characterized by a minimal molar ellipticity at 220 nm. The $F(ab)_2'$-Ig fragment induced by pseudopeptides ψ-439 (Met^{51}-Val^{52}) and ψ-440 (Lys^{50}-Met^{51}) clearly kept such structural profile. As above presented, the $F(ab)_2'$ induced by the ψ-440 (Lys^{50}-Met^{51}) possess the highest β-strand content when its secondary structure data were deconvoluted. Some how a given and specific geometrical complementarity could be more feasible if an appropriately folded $F(ab)_2'$ antibody fragment docks properly to its specific ligand as complementary molecule on the *Plasmodium* parasite surface allowing the parasite neutralization.

In summary, passive transfer of $F(ab)_2'$ antibody fragments induced against site-directed designed isoster bond reduced amide MSP-1 pseudopeptides, can be considered a promising strategy for controlling malaria infection in a real background, as shown herein in mice, and might have important implications for malaria treatment in humans and for establishing novel malaria vaccine design strategies.

5. Conclusions

Malaria is still gaining importance among all transmissible diseases mainly due to it provokes a negative impact in economy and public health, in addition is getting expanded through the world. In consequence searching for potent synthetic vaccines and novel therapeutical strategies for controlling malaria becomes as an urgent need. Among these novel strategies, designing potential bioactive molecules in a site-directed fashion, will allow obtaining highly specific antibody reactivity directed to specific pathogen ligands to be efficiently blocked. This new kind of molecular weapons should be able to induce neutralizing antibodies having strong functional properties to avoid the *in vivo* infection and the subsequent disease. In a previous work we have obtained evidence that passively transferring an entire Ig molecule to an infected animal model of the same specie, conferred protection against malaria. In the present work we have demonstrated that a methylene amine ψ-[CH_2NH] isoster bond replacement in the target malaria antigen, have specifically directed the antibody stimulation reactivity to the *C*-terminal portion of the parent antigen's aminoacid sequence, being in this case the MSP-1^{51-61} the possible B-epitope and its geometrically defined induced antibody $F(ab)_2'$ fragments conferred a precise parasite blocking effect.

In consequence, passively transferring $F(ab)_2'$-antibody fragments induced in a given animal species to another, being these antibodies induced against specific site-directed designed antigens such as peptide-bond modified sequences so-called pseudopeptides, constitutes a potential therapeutical strategy to be further considered in the treatment of malaria infections.

Acknowledgment

This research has been supported by the Asociación de Investigación Solidaria-SADAR, Pamplona, Spain and the Agencia Española de Cooperación Internacional para el Desarrollo-AECID, Madrid, Spain. *Plasmodium yoelii* 17XL was a kind gift from Prof. Lilian Spencer Valero from the Cellular Biology Department, Universidad Simón Bolívar, Caracas, Venezuela. We would like to thank Yahson Fernando Varela for his help with Circular Dichroism experiments and to Nora Martinez and Gisselle Rivera for helping with the translation of the manuscript. Special thanks are given to Magda Bohorquez for technical support and Armando Moreno-Vranich for some figure designing.

References

Bennett, K.L., Smith, S.V., Truscott, R.J., Sheil, M.M., 1997. Monitoring papain digestion of a monoclonal antibody by electrospray ionization mass spectrometry. Anal. Biochem. 245, 17–27.

Boyle, D.B., Newbold, C.I., Smith, C.C., Brown, K.N., 1982. Monoclonal antibodies that protect in vivo against Plasmodium chabaudi recognizes a 250,000-dalton parasite polypeptide. Infect. Immun. 38:, 94–102.

Clamp, M., Cuff, J., Searle, S.M., Barton, G.J., 2004. The Jalview Java alignment editor. Bioinformatics 20 (3), 426–427.

Cushman, M., Oh, Y.I., 1991. Development of methodology for the synthesis of stereochemically pure Phe-ψ[CH_2N]Pro linkages in HIV protease inhibitors. J. Org. Chem. 56, 4161–4167.

Espinal, C., Guerra, P., Olaya, P., 1982. Isolation and characterization of Colombian *Plasmodium falciparum* strains. Biomédica 2, 118–128.

Green, T.J., Kreier, J.P., 1978. Demonstration of the role of cytophilic antibody in resistance to malaria parasites (*Plasmodium berghei)* in rats. Infect. Immun. 19, 138–145.

Gregory, L.M., Theresa, M.T., Dennis, B.R., 2003. Purification of antibody Fab and F (ab')$_2$ fragments using Gradiflow technology. Protein Expres. Purif. 32 (1), 135–140.

Ho, P.T., Chang, D., Zhong, J.W., Musso, G.F., 1993. An improved low racemization solid-phase method for the synthesis of reduced dipeptide (ψ CH_2NH) bond isosteres. J. Pept. Res. 6, 10–12.

Holder, A., Blackman, M., Burghaus, P., Chappel, J., Ling, I., McCallum-Deighton, N., Shai, S., 1992. A malaria merozoite surface protein (MSP-1) structure, processing and function. Mem. Inst. Oswaldo Cruz 87 (Suppl. III), 37–42.

Houghten, R.A., 1985. General method for the rapid solid-phase synthesis of large numbers of peptides: specificity of antigen–antibody interaction at the level of individual amino acids. Proc. Natl. Acad. Sci. U.S.A. 82, 5131–5135.

Janse, C., Waters, A., 1995. The *Plasmodium berghei* Research Model of Malaria. Chapter 2. Introduction to *Plasmodium berghei*.

Jouin, H., Rogier, C., Trapa, J.F., Mercereau-Puijalon, O., 2001. Fixed, epitope-specific, cytophilic antibody response to the polymorphic block 2 domain of the *Plasmodium falciparum* merozoite surface antigen MSP-1 in humans living in a malaria-endemic area. Eur. J. Immunol. 31, 539–550.

Kaufmann, B., Nybakken, G.E., Chipman, P.R., Zhang, W., Diamond, M.S., Fremont, D.H., Kuhn, R.J., Rossmann, M.G., 2006. West Nile virus in complex with the Fab fragment of a neutralizing monoclonal antibody. Proc. Natl. Acad. Sci. U.S.A. 103 (33), 12400–12404.

Kauth, C.W., Epp, C., Bujard, H., Lutz, R., 2003. The merozoite surface protein, 1 complex of human malaria parasite *Plasmodium falciparum*: interactions and arrangements of subunits. J. Biol. Chem. 278 (25), 22257–22264.

Lambros, C., Vanderberg, J.P., 1979. Synchronization of plasmodium falciparum erythrocytic stages in culture. J. Parasitol. 65, 418–420.

Lioy, E., Suarez, J., Guzman, F., Siegrist, S., Pluschke, G., Patarroyo, M.E., 2001. Synthesis, biological, and immunological properties of cyclic peptides from Plasmodium falciparum merozoite surface protein-1. Angew. Chem. Int. Ed. Engl. 40, 2631–2635.

Lozano, J.M., Espejo, F., Díaz, D., Salazar, L.M., Rodríguez, J., Pinzón, C., Calvo, J.C., Guzmán, F., Patarroyo, M.E., 1998. Reduced amide pseudopeptide analogues of a malaria peptide possess secondary structural elements responsible for induction of functional antibodies which react with native proteins expressed in *Plasmodium falciparum* erythrocyte stages. J. Pept. Res. 52, 457–469.

Lukasz, K., Black, C.G., Goschnick, M.W., Stowers, A.W., Coppel, R.L., 2002. Immunization with a combination of merozoite surface proteins 4/5 and 1 enhances protection against lethal challenge with *Plasmodium yoelii*. Infect. Immun. 70 (12), 6606–6613.

Majarian, W.R., Daly, T.M., Weidanz, W.P., Long, C.A., 1984. Passive immunization against murine malaria with an IgG3 monoclonal antibody. J. Immunol. 132, 3131–3137.

Martínez, P., Yandar, N., Lesmes, L.P., Forero, M., Pérez-Leal, O., Patarroyo, M.E., Lozano, J.M., 2009. Passive transfer of *Plasmodium falciparum* MSP-2 pseudopeptide-induced antibodies efficiently controlled parasitemia in *Plasmodium berghei*-infected mice. Peptides 30, 330–342.

Merrifield, R.B., 1963. Solid phase peptide synthesis. I. The synthesis of a tetrapeptide. J. Am. Chem. Soc. 85, 2149–2154.

Miller, L., Roberts, T., Shahabuddin, M., McCutchan, T., 1993. Analysis of sequence diversity in the *Plasmodium falciparum* merozoite surface protein-1 (MSP-1). Mol. Biochem. Parasitol. 59, 1–14.

Ramos-Avila, A., Gallegos, J.L., Dehesa Zentella, A., Rodríguez Machuca, C., Altamirano-Moreno, M.M., Narvaéz, V., Herrera-Legorreta, M., 2007. Immunomodulatory role of chloroquine and pyrimethamine in *Plasmodium yoelii* 17XL infected mice. J. Immunol. 65, 54–62.

Sasaki, Y., Murphy, W.A., Heiman, M.L., Lance, V.A., Coy, D.H., 1987. Solid-phase synthesis and biological properties of ψ[CH_2NH] pseudopeptide analogues of a highly potent somatostatin octapeptide. J. Med. Chem. 30, 1162–1166.

Smythe, J.A., Coppel, R.L., Brown, G.V., Ramasamy, R., Kemp, D.J., Anders, R.F., 1988. Identification of two integral membrane proteins of *Plasmodium falciparum*. Proc. Natl. Acad. Sci. U.S.A. 85, 5195–5199.

Spencer, L.M., Quintana, D., Hidalgo, L., 2008. Evaluation of the inhibition of invasion *in vitro* of *P. yoelii* strain with different monoclonal antibodies raised against MSP-119. Rev. Biomed. 19, 45–51.

Spencer, L.M., Ogun, S.A., Fleck, S.L., Ling, I.T., Scott-Finnigan, T.J., Blackman, M.J., 1998. Passive immunization with antibodies against three distinct epitopes on *Plasmodium yoelii* merozoite surface protein 1 suppresses parasitemia. Infect. Immun. 66 (8), 3925–3930.

van der Heyde, H.C., Elloso, M.M., vande Waa, J., Schell, K., Weidanz, W.P., 1995. Use of hydroethidine and flow cytometry to assess the effects of leukocytes on the malarial parasite *Plasmodium falciparum*. Clin. Diagn. Lab. Immunol. 2, 417–425.